7 SCIENTIFIC HIGHLIGHT OF THE MONTH: *Ab initio* Study of Magnetoelectricity in Composite Multiferroics

M. Fechner[1], I.V. Maznichenko[2], S. Ostanin[1], A. Ernst[1], J. Henk[1], I. Mertig[1,2]
[1]Max-Planck-Institut für Mikrostrukturphysik, Weinberg 2, D-06120 Halle, Germany
[2]Martin-Luther-Universität Halle-Wittenberg, Fachbereich Physik, D-06099 Halle, Germany

Abstract

The coexistence of magnetism and ferroelectricity in the same crystalline phase of a so called multiferroic material involves the opportunity of magneto-electric coupling. Magnetoelectric coupling, however is highly attractive since it offers magnetization switching by an electric field or polarization switching by a magnetic field. Since this phenomenon, in principle, allows to store information in nanometer-sized memories with four logic states, the issues of multiferroics (MF) are of prime interest. Studies based on density functional theory have significantly contributed to this rapidly developing field of single-phase MF (see, Ψ_k Scientific Highlight 92 by S. Picozzi and C. Ederer and references therein). In such multiferroics, however, the electric polarization and magnetization interact weakly with each other while ferromagnetism disappears far below room temperature. A more robust scenario of magnetoelectricity might occur in artificial MF composed of ferromagnetic thin films which are grown epitaxially on a ferroelectric substrate. Inaccessible by conventional synthesis, composite multiferroics exhibit specific properties which are superior to those of customary materials. In the study of composite multiferroics, the results of *ab initio* calculations, reported by Tsymbal's group from Nebraska University after 2006, have shown an extremely promising direction for the next years. Although these calculations go ahead of experiment they explore the trends and basic physics of magnetoelectrics. Here, on the basis of first-principles calculations we predict that epitaxial ultrathin Fe films deposited on TiO_2-terminated (001) surface of $A\mathrm{TiO}_3$ perovskites (A = Pb, Ba) exhibit an unexpected change in their magnetic structure with increasing Fe-film thickness. The magnetic order changes from strongly ferromagnetic for the single-monolayer-Fe system to ferrimagnetic with almost vanishing magnetization upon deposition of a second Fe layer. Ferromagnetic order is restored for thicker Fe films. This effect can be understood in terms of hybridization of electronic states and structural relaxation. Additionally, we study the effect of iron oxidation on the magnetoelectric coupling at the $\mathrm{Fe}_2/A\mathrm{TiO}_3(001)$ interface. The simulated oxygen coverage ranged between 0.5 and 2.0 adsorbed O atom per Fe atom, using a slab geometry. The magnetic properties of the Fe layer are gradually degraded with increasing O coverage for $c > 1.5$. However, the change in magnetization which is induced by the electric polarization reversal remains robust for all energetically favorable compositions. For instance, we show that the surface oxidation of composite MF cannot destroy the switchable magnetoelectricity.

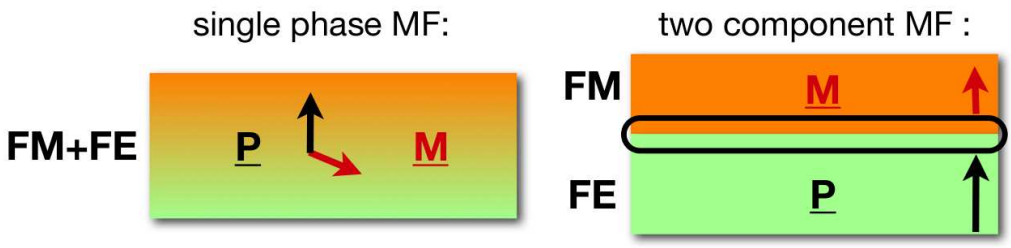

Figure 1: Single-phase and composite multiferroics are sketched in the left and right panels, respectively. In the single-phase MF, its magnetoelectricity is the volume effect while for composite multiferroic, in contrary, the ME coupling is confined to the interface area.

1 Introduction

When any two of all four primary ferroic properties, i. e., ferroelectricity, ferromagnetism, ferroelasticity, and ferrotoroidicity coexist in a so called multiferroic material (MF), its symmetry must be restricted dramatically [1]. In the absence of space-inversion and time-reversal symmetry, the occurrence of ferroelectricity and magnetism in the same phase of an MF allows the observation of both a switchable electric polarization, $\boldsymbol{P}$, and a switchable magnetization, $\boldsymbol{M}$. In principle this phenomenon allows to store information in nanometer-sized memories with four logic states [2–4].

Although some single-phase MFs, such as $BiFeO_3$ and $R MnO_3$ (R rare earths), were known since mid of the seventies [5], the search for novel multiferroics is not finished yet. Moreover, their classification has been revised [6] since 2003 when the type-II class of magnetic MF has been established. For instance, in $TbMnO_3$ ferroelectricity is caused by a particular type of magnetic order, which exists only at low temperature. In multiferroics, no matter what its class, an applied electric field, $\boldsymbol{E}$, displacing the magnetic ions, affects the magnetic exchange coupling or, vice versa, the external magnetic field, $\boldsymbol{H}$, induces the electric polarization: $P_i \sim \alpha_{ij} H_j$, where α is the magnetoelectric tensor and $i, j = x, y, z$. According to Landau theory, the linear magnetoelectric (ME) contribution to the Gibbs free energy is $E_i \alpha_{ij} H_j$. If α is sufficiently strong then $\boldsymbol{M}$ can be easily modified by $\boldsymbol{E}$. It should be kept in mind that magnetoelectricity is a volume effect for which the induction of $\boldsymbol{M}$ depends linearly on $\boldsymbol{E}$. In a type-I single-phase MF, $\boldsymbol{P}$ and $\boldsymbol{M}$ interact weakly and, therefore, α is marginal there. Besides, all multiferroics possess a hierarchy of phase transformations [7], in which ferromagnetism disappears far below room temperature. In a type-II MF, the magnitude of $\boldsymbol{P}$ is never large, which precludes strong magnetoelectricity. Obviously, the quest for fundamentally new multiferroics requires a better understanding of the mechanisms which mediate the ME coupling.

Ab initio calculations based on density functional theory (DFT) predict that a voltage of about 30 meV, applied across a $SrRuO_3/SrTiO_3$ interface, without magnetic cations, can induce a net magnetic moment [8]. Since the space-inversion symmetry is broken between the two unlike terminations, the ME effect results entirely from spin accumulation at the interface. The effect might be enhanced by the use of materials with higher spin polarization. Indeed, a more robust scenario of magnetoelectricity occurs in epitaxially grown two-phase MF consisting of ferroelec-

tric and ferromagnetic components. The ME effect is mediated by strain across the biferroic interface. Inaccessible by conventional synthesis, the MF composites exhibit specific properties which are superior to those of customary materials. *Ab initio* studies suggest that the interface bonding is the source of strong ME coupling in $Fe/BaTiO_3(001)$ [9,10]. The interfacial Ti atoms show an induced magnetic moment of about $0.3\,\mu_B$. Moreover, for the two opposite directions of $\boldsymbol{P}$ ($P_\downarrow$ and $P_\uparrow$), there are rather noticeable differences of 0.1–0.2μ_B in the magnetic moments of Fe and Ti at the interface. This is a very promising phenomenon, which is entirely confined to the ferroelectric/ferromagnetic interface and which differs from the volume ME effect. The interface ME effect defines the change in magnetization at the coercive field E_c: $\mu_0\Delta M \approx \alpha E_c$. α of about $2 \cdot 10^{-10}\,\mathrm{Gcm^2/V}$ estimated for $Fe/BaTiO_3(001)$ from first principles, is two orders of magnitude larger than that predicted for $SrRuO_3/SrTiO_3$.

Epitaxial growth of the two-pase MF thin films of high quality continues to be very challenging. A 30 nm thick Fe(001) film has been grown recently on a ferroelectric $BaTiO_3(001)$ substrate [11]. For this MF, the interface ferromagnetic resonance mode is characterized by a large out-of-plane magnetic anisotropy comparable to and of opposite in sign to the shape anisotropy, the latter favoring an in-plane easy axis for thick film interiors. The trends of magnetic anisotropy detected for $Fe/BaTiO_3$ are in a good agreement with corresponding *ab initio* calculations [10, 12]. In the case of one Fe monolayer (ML), DFT predicts that perpendicular anisotropy is favored to in-plane anisotropy by 0.72 meV (0.54 meV) per Fe atom for $P_\downarrow$ ($P_\uparrow$) [10]. Although the spin reorientation transition under switching of $\boldsymbol{P}$ is not found from first principles, the ME coupling alters the magnetocrystalline anisotropy energy by about 50 %. The magnetic order of $Fe/BaTiO_3$ can be tuned by the Fe layer thickness to ferrimagnetic with almost zero $\boldsymbol{M}$ upon deposition of a second Fe ML [10]. Ferromagnetic order is restored for Fe films thicker than 3 ML, for which the shape anisotropy energy favors in-plane alignment of $\boldsymbol{M}$ [12].

Recently, Niranjan *et al.* [13] modeling different $Fe_3O_4/BaTiO_3(001)$ interfaces within DFT, have found that ME coupling is stronger for the O-deficient type of the Fe_3O_4 interface. This suggests that the presence of oxygen or oxygen vacancies at the biferroic interface plays an important role. The temperature dependent magnetization curves of epitaxial magnetite films grown on $BaTiO_3(001)$ demonstrate [14] a strong perpendicular magnetic anisotropy, which is modified by the piezoelectric response of the substrate.

2 Magnetoelectric coupling in Fe/BTO

In the following we give a detailed example of the magnetoelectric coupling at an interface. For that reason we present results obtained from first-principles calculations [10]. A perfect model system for a multiferroic interface is an $ATiO_3$ (A = Ba or Pb) substrate covered with iron layers 3. Both materials are not only ferroic separately at room temperature but also as a two-component compound. The polarization of the FE substrates ranges from $26\,\mu\mathrm{C/cm^2}$ for BTO to $75\,\mu\mathrm{C/cm^2}$ for PTO; iron has a magnetic moment of $2.25\,\mu_B$. More importantly, the in-plane lattice constants of the [001] surfaces of the substrates match nearly perfectly with that of iron. The mismatch $(a_{\mathrm{sub}} - a_{\mathrm{Fe}})/a_{\mathrm{sub}}$ is below 3 % and allows epitaxial growth of the interface, as has recently been shown experimentally [11].

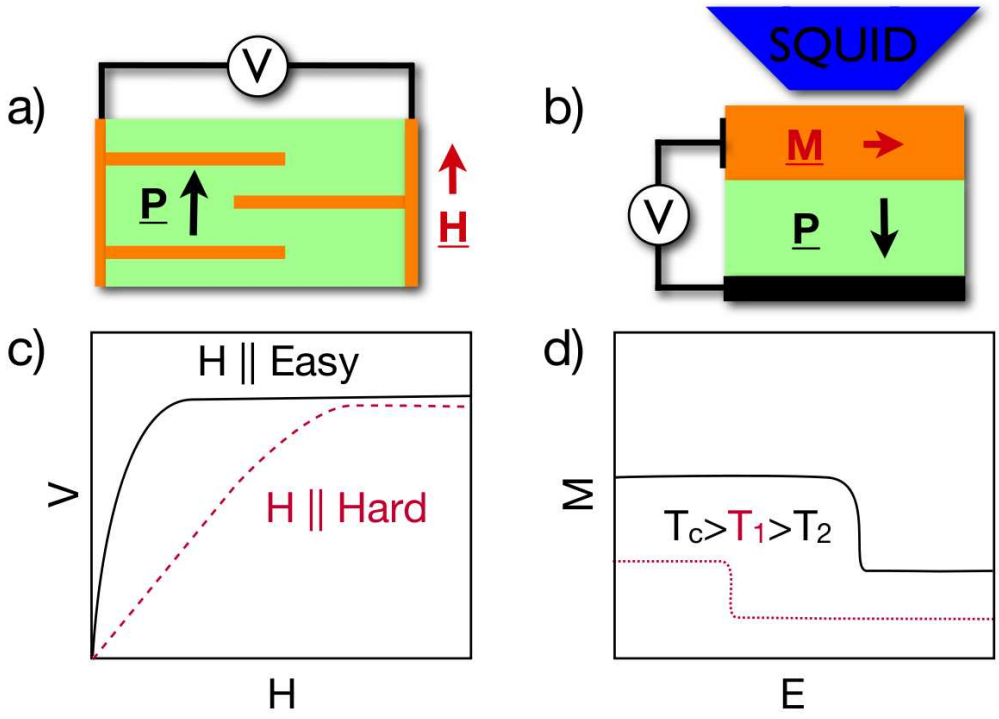

Figure 2: The schemes a and b in the upper panel show experimental setups for determining the ME coupling at biferroic interfaces. The figures below show the corresponding results of the measurements. In a) Ni contacts are embedded in a $BaTiO_3$ matrix and an applied magnetic field gives rise to a voltage change. In b) a $La_{1/3}Sr_{2/3}MnO$ film is deposited on top of a $BaTiO_3$ surface. SQUID allows the detection of the film magnetization under an applied bias. A detailed discussion of both experiments is given in [2, 15].

To treat the interplay between geometric, electronic and magnetic properties in the best way we use a multi-code approach. The geometric relaxations and magnetic properties are obtained by the Vienna Ab-initio Simulation Package (VASP) [16]. A cross-check of the magnetic structure obtained by VASP was done with the scalar-relativistic Korringa-Kohn-Rostoker (KKR) [17] method; the magnetocrystalline anisotropy was additionally computed with a relativistic layer-KKR code [18]. In all codes the local spin-density approximation (LSDA) to density-functional theory (DFT) is used. Further various quantities were carefully compared among the three computer codes to obtain consistent results. Reliability is achieved by numerous convergence tests.

At the atomic scale both materials are combined via the Fe/TiO_2 interface. The TiO_2 termination of the FE substrate was chosen since it is energetically preferable [19]. The same arguments hold for the positions of the Fe atoms which prefer to sit above the oxygen atoms. To model the change of the polarization direction the structural properties of the FE substrate have to be considered. Within the tetragonal phase the polarization of the $ATiO_3$ is caused by the displacement of the atoms along the [001] axis. It can be defined as $\delta \equiv z(\text{cation}) - z(\text{O})$. For the considered systems there exist two distinguished scenarios for the atomic displacements. If the displacement in the FE substrate is positive the polarization points towards the interface; if it is negative, the polarization points away from the interface. Both situations mimic the state after polarization switching, that is in remanence. We denote the two states corresponding their polarization directions as $P_\uparrow$ and $P_\downarrow$. For our calculation they are modeled by considering two different supercells. Both consist of 5 unit cells of $ATiO_3$ (A = Ba or Pb) covered with L monolayers of iron and separated by 2 nm of vacuum. They differ in δ, which was set to the positive bulk value for the $P_\uparrow$ state and negative for $P_\downarrow$. The structural relaxation concerns the three top layers of the $ATiO_3$ and the Fe layer until the forces are less than 5 meV/Å.Å

The magnetic and ferroelectric properties are shown in Fig. 3. On the left-hand side of Fig. 3 the unit cell of $Fe_2/TiO_2/PbTiO_3(001)$ with $P_\uparrow$ is shown. For the distance between the TiO_2 and Fe at the interface we obtained—after structural relaxation independently on the iron thickness and polarization direction—a value of $a \approx 1.8$ Å. Further compression of the surface area of $ATiO_3$, which could suppress ferroelectricity, was not found. The only structural detail which is sensitive to the number of iron layers is the distance between the first and second iron layer. In case of two layers (not shown in the figure) this distance is about 1.05 Å whereas for thicker layers it is about 1.2 Å. Later we will explain the change in the magnetic ordering caused by the structural relaxation. A detailed overview of the structure is given in [10].

At the right-hand side of Fig. 3 the two order parameters at the interface of $Fe_2/TiO_2/PbTiO_3(001)$ are shown. The unit-cell resolved polarizations were calculated by $P_i = \delta \cdot q_{\text{Born}}$, where q_{Born} is the Born effective charge. At first glance, it is clearly visible that the largest interference of the two ferroic properties is found in the TiO_2 layer. In particular there the magnetization changes sign when the polarization is turned. A change of the polarization due to the vicinity of the iron was not observed. Similarly the iron moments are only mildly influenced by the change of the polarization direction. The total change of magnetization $\Delta M = M(P_\downarrow) - M(P_\uparrow)$ for this system is about 1 μ_B. This change will be explained by a detailed analysis of the hybridization

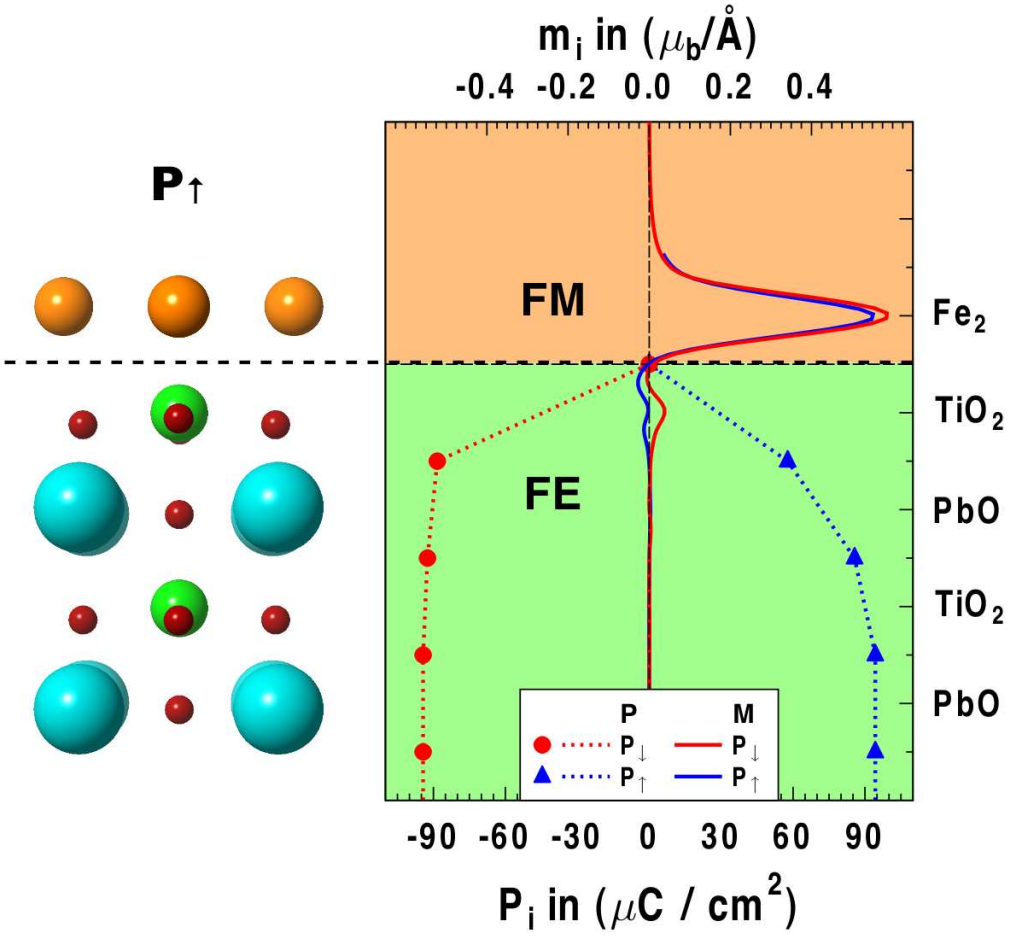

Figure 3: The unit cell of biferroic $Fe_2/TiO_2/ATiO_3(001)$ (A = Ba, Pb) with a 2 nm thick vacuum layer is sketched as a side view. On the right-hand side the order parameters at the interface for 1 ML Fe on top of PTO are shown. The layer resolved polarization is plotted as a dotted line, whereas the magnetization is represented by a solid line. The two colors correspond to the states $P_\uparrow$ (blue) and $P_\downarrow$ (red). The largest change of the magnetization was obtained within the TiO_2 plane next to the interface.

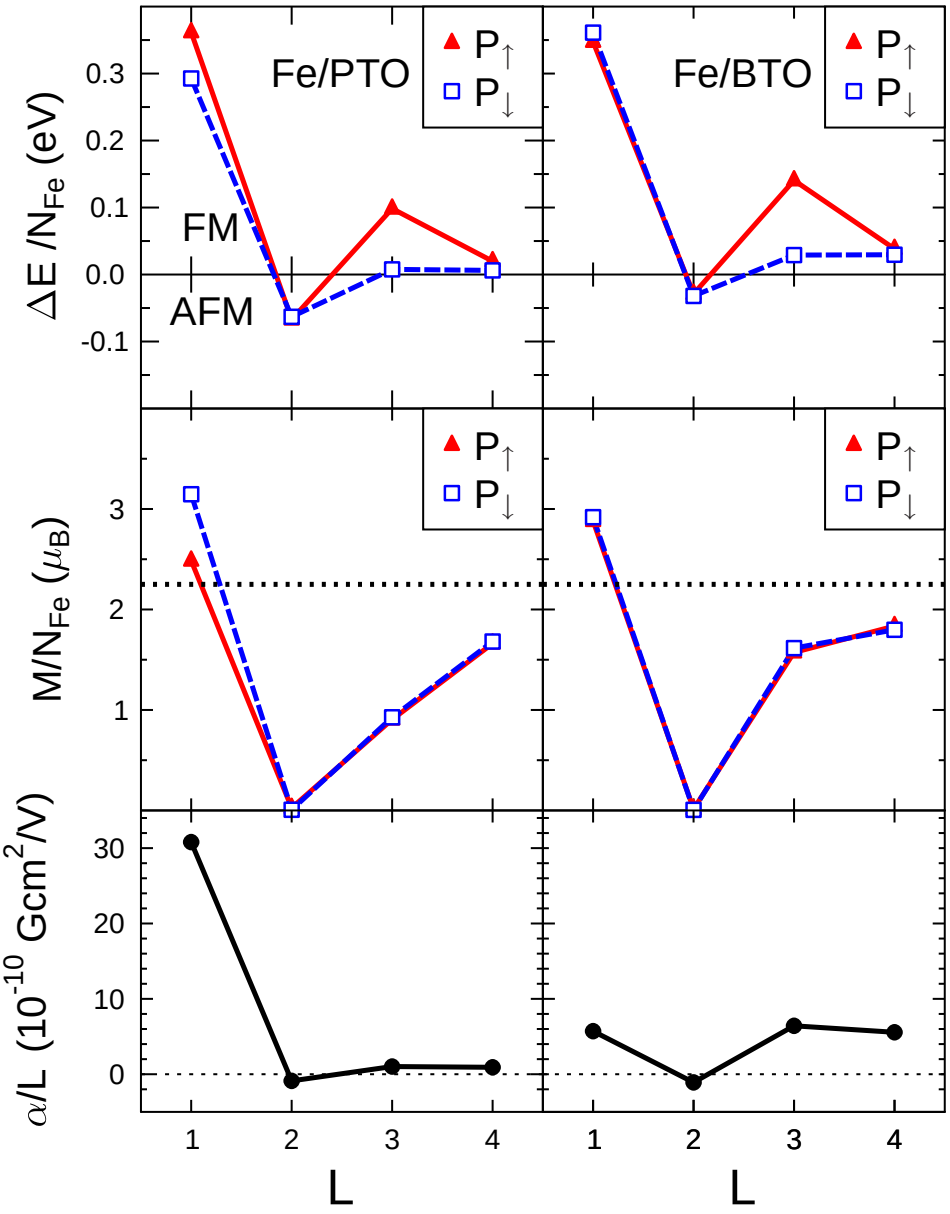

Figure 4: Magnetism of $(Fe_2)_L/ATiO_3(001)$ for $PbTiO_3$ (PTO) and $BaTiO_3$ (BTO) versus Fe-film thickness L. In the top panel the total-energy difference $\Delta E \equiv E_{\rm AFM} - E_{\rm FM}$ of the antiferrimagnetic (AFM) and ferromagnetic (FM) configurations are normalized with respect to the number $N_{\rm Fe}$ of Fe atoms in the film unit cell. In the middle panel the magnetization per Fe atom for the lowest-energy configuration is plotted. Here, the dotted line indicates the magnetic moment of Fe bulk. The magnetoelectric coupling coefficient α of $(Fe_2)_L/ATO(001)$ (A = Ba, Pb) is plotted versus the Fe-film thickness L in the lower panel.

of Fe, Ti and O atoms at the interface in Section 2.1.

For all substrates and Fe-film thicknesses, total energies of two magnetic configurations were computed: ferromagnetic (FM) and antiferrimagnetic (AFM) ordering was considered. The top panel in Fig. 4 shows the energy difference $\Delta E = E_{\mathrm{AFM}} - E_{\mathrm{FM}}$ between these two configurations. For both substrates we obtained for 1ML Fe ferromagnetic order of the iron independently of the polarization direction. Adding a second layer changes the ordering substantially. Here, an antiferromagnetic ordering seems to be preferred. But the constrained self-consistent calculations did not converge towards a complete AFM configuration; forcing the top layer to be antiferromagnetic the layer beneath always shows ferromagnetic order with suppressed moments. Consequently the preferred order for $L = 2$ is antiferrimagnetic. Deposition of a third Fe layer restores the ferromagnetic order. In almost all cases, the relation of $E_{\mathrm{FM}} < E_{\mathrm{AFM}}$ is obtained. An exception is $L = 2$ for which it was not possible to reach an antiferromagnetic solution but an antiferrimagnetic instead. Thus, the magnetic order of the two-phase multiferroics can be tuned by the Fe-film thickness independently of the perovskite substrate. Strain and electric polarizability are of minor importance for the ordering.

The middle panel of Fig. 4 shows the magnetization of the interface as a function of the iron layer thickness. The magnetization is normalized to the number of iron atoms to allow comparison of the results. The two curves within the figures correspond to the two polarization states, and their difference is the change of magnetization under polarization reversal. For 1 ML iron on PTO there exists a large magnetization which is mainly carried by the magnetic moments of iron $m_{\mathrm{Fe}} \approx 3\,\mu_{\mathrm{mathrmB}}$. A difference of about $1\,\mu_{\mathrm{B}}$ between the two polarization directions is obvious in the case of Fe on PTO. This is in contrast to the BTO substrate where this difference is tiny ($\Delta M = 0.05\,\mu_{\mathrm{B}}$). With two layers of iron the magnetization drops down to almost zero due to the change of the abovementioned magnetic order. Further, the two curves lie on top of each other. Upon adding more layers ferromagnetic order is stabilized and the magnetization increases. For more layers the magnetization converges towards the bulk value of iron (dashed line).

Based on the change of the magnetization the surface magneto-electric coefficient is calculated. It is defined as $\alpha_{\mathrm{surf}} = \Delta M/(E_c \cdot A)$, where A is the surface area and E_c is the coercive field needed to switch the polarization. Using the experimental values of E_c for BTO (10 kV/cm) and PTO (33 kV/cm), the coupling coefficients were calculated and plotted as a function of the number of iron layers in the lower panel of Fig. 4. Since the ΔM is largest for Fe on PTO, the largest coupling is obtained for this system. Interestingly the coefficient for PTO decays with increasing number of iron layers. This is in contrast to BTO where α_{surf} stays nearly constant. An exception is the case $L = 2$ for which the value approaches zero for both substrates. Theoretical studies of superlattices of BTO and Fe show that this value is also valid for thick Fe films [9]. To compare these values we consider values obtained for a $SrRuO_3/SrTiO_3$ interface. *Ab initio* calculations based on the density functional theory (DFT) predict that a voltage of about 30 meV/e, applied across the interface without magnetic cations, can induce a net magnetic moment [8]. This leads to an α_{surf} two orders of magnitude smaller than that predicted for the Fe/PTO system.

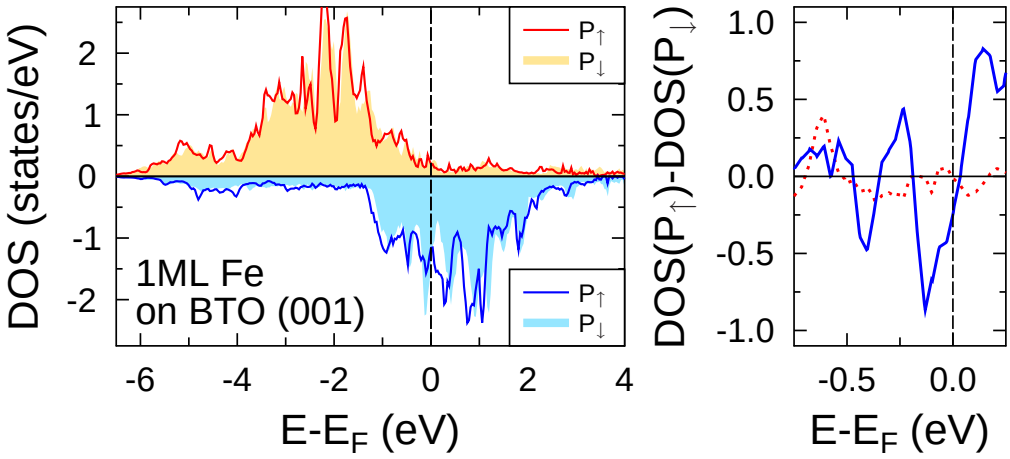

Figure 5: Electronic structure at the surface of $(Fe_2)_1/BaTiO_3(001)$. The left panel shows the spin-resolved density of states (DOS) for Fe/BTO. The right panel gives the difference between the spin-resolved DOS for $P_\uparrow$ and $P_\downarrow$ close to the Fermi energy E_F (majority: red, dotted; minority: blue, solid).

2.1 Microscopic origin of ME coupling

From the preceding it is evident that the magnetic moments of the Fe film are changed in a complex manner by the interface. To achieve insight into the mechanism, we illustrate in Fig. 5 the spin-polarized electronic properties at the Fe/BTO interface. A switching effect is mainly seen for the minority electrons around the Fermi energy. This effect is much more obvious in the difference between the two densities for the two polarizations. The effect is clearly dominating for minority electrons whereas there are only minor changes for majority electrons. This could be attributed to a hybridization of the Fe d-minority states with the Ti d-states which leads to an induced moment on the Ti site oriented opposite to the iron moments. Since the Ti atom is closer to the Fe atoms in the $P_\uparrow$ state the hybridization is stronger for this configuration. Consequently the induced Ti moment is larger. For $P_\downarrow$ the opposite is the case and a smaller Ti moment can be observed. It turns out that it this moment which causes the difference of the total magnetization between the two polarization states.

Because of the larger displacement of the atoms this effect is even more pronounced in Fe/PTO (confer the right-hand side of Fig. 3). In contrast to BTO an additional large induced moment on the oxygen could be observed in the $P_\downarrow$ case. The O moment is aligned parallel with the iron moments. Switching to $P_\uparrow$ causes in induced moment on Ti antiparallel to the iron moments which then induces a moment on the lower oxygen. The larger displacement and the additionally induced moment causes the sizable change of $1\,\mu_B$.

The change of the minority charge distribution in real space is shown in Fig. 6 for Fe on BTO. Considering the right-hand-side panel, it is obvious that most of the minority charge is pushed into the interstitial region between the iron atoms under polarization switching. This charge originates mainly from the Ti atom, as is evident from the side view, and is responsible for the

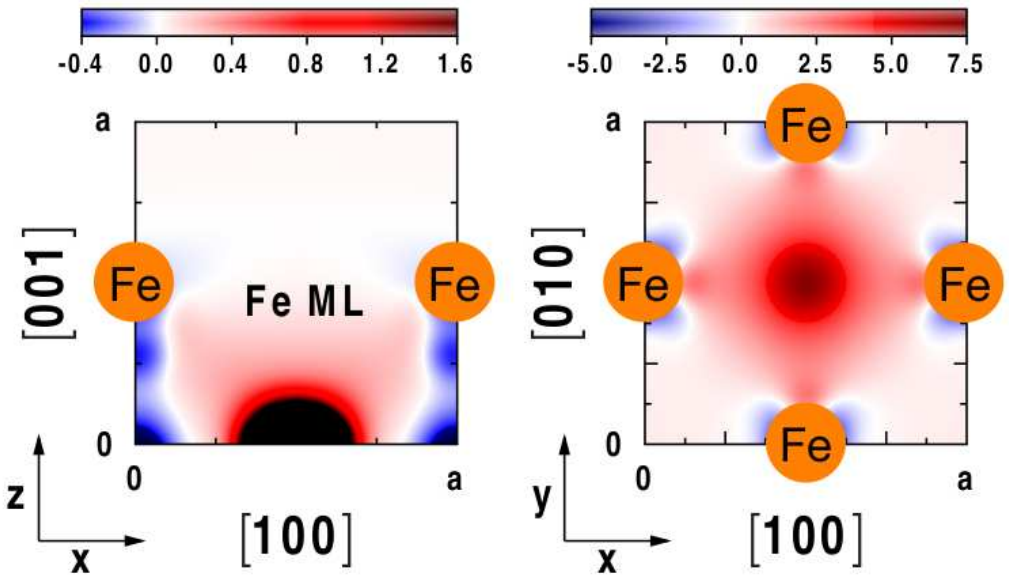

Figure 6: (Color) Charge redistribution of minority-spin electrons at the interface of $(Fe_2)_1$/BTO(001) upon reversal of the electric polarization $\boldsymbol{P}$ with respect to the surface normal. The difference of the charge densities for $P_\uparrow$ and $P_\downarrow$ is depicted in a perpendicular (left) and an in-plane cut through the Fe atoms (size a^2; color scales in arbitrary units). The Fe atoms are represented by spheres.

change of magnetization under switching.

While the magnetic moments do not change sign upon $\boldsymbol{P}$ reversal, we consider the possibility of a spin-reorientation transition as another type of magnetoelectric switching. To investigate this mechanism we were using the relativistic layer-KKR, the magnetic anisotropy for $(Fe_2)_1$/BTO(001) is computed within the framework of the magnetic force theorem [20]. For both P orientations perpendicular anisotropy is favored with respect to in-plane anisotropy, namely by 0.72 meV ($P_\downarrow$) and 0.54 meV ($P_\uparrow$) per Fe atom. It worth mentioning that the anisotropy energies are twice as large as in FePt [21,22]. In summary we find a change of the magnetization upon polarization reversal but no change of the magnetization direction.

2.2 Magnetic order

As previously mentioned, the magnetic order changes as a function of the Fe-layer thickness. In particular the magnetic order of two Fe layers becomes antiferrimagnetic (Fig. 4). For two layers the magnetic moments in the Fe interface layer are almost quenched while the sizable moments in the surface layer are ordered antiparallelly. This is due to the small distance of 1 Å between the iron layers. Since the two Fe sites in the top layer are inequivalent, e. g. Fe is on top of Ti (Ba) sites. They carry different magnetic moments; this reflects the environment of these atoms, in particular the atomic volumes and the hybridization. Polarization reversal affects mainly the positions of Ti atoms and consequently those of the Fe atoms atop. The small volume of interfacial Fe is reduced even further and leads to very small magnetic moments. The small size of Fe atoms in the interface layer explains as well the antiferromagnetic ordering of

their local magnetic moments [23]. Adding a third Fe layer increases both the coordination numbers and the atomic volumes and consequently restores ferromagnetic order.

2.3 Oxygen coverage

So far, our *ab initio* studies of MF composites were focused on perfect interfaces without oxidants. However, the strength of the ME coupling may be sensitive to the degree of oxidation. The Fe oxidation is unavoidably motivated, firstly, by the growth process of the ferroelectric since oxygen will react with the iron during Fe growth. Secondly, for the uncovered Fe films further oxidation occurs when the sample is removed from the chamber. These two possible scenarios may result in some particular Fe-O compositions which vary from highly oxidized Fe to an almost clean surface. Thus, the *ab initio* based modeling would be extremely useful. In the following, we study from first principles the key electronic, magnetic and structure factors behind the oxidation process of the 1-ML Fe grown on $BaTiO_3(001)$ and $PbTiO_3(001)$. We demonstrate in which positions oxygen adatoms sit above the Fe layer and that the ME coupling in these composites is robust against the O composition.

The equilibrium bond length calculated for molecular O_2 is 1.23 Å. For $Fe_2/TiO_2/ATiO_3(001)$, the in-plane lattice parameter is about 3.9 Å, while the Fe-Fe separation is about 2.75 Å. The latter is two times larger than that of the O_2 dissociation. Therefore, to model the Fe oxidation of Fe/BTO and Fe/PTO we must consider O coverages, $c(O_x : Fe_2)$, ranging between $c = 1/2$ and two adsorbed O atoms per Fe atom ($c = 2$). There are twelve possible configurations for these coverages [Fig. 7(c)]. For $c = 0.5$, one oxygen adatom per unit cell can occupy the site either above A or above Ti or, alternatively atop Fe. For $c = 1$, the two O adatoms form four configurations marked in Fig. 7(c) as AT, AF, TF and FF. In the case of $c = 1.5$, we relax the ATF, TFF and AFF configurations. And, finally, for $c = 2$ there are two more possibilities to distribute four adatoms, such as ATFF (the case of full coverage) and 4H, which means that all four hollow sites are occupied by O. Using a $10 \times 10 \times 6$ Monkhorst-Pack [24] mesh for the Brillouin-zone integration, we relaxed the O adatoms and Fe atoms plus all atoms of the two top ABO_3 unit cells until the forces were less than $1.0 \cdot 10^{-2}$ eV/Å. After relaxation, oxygen forms an overlayer above the Fe layer, with the distance depending on coverage and direction of $\boldsymbol{P}$.

In the case $c = 0.5$, the most favorable configuration is A. However, the configurations A and T can coexist for this O coverage since the difference in energy between them is $E_T - E_A \sim 0.2$ eV. For the ABO_3 substrates, the energetics are almost the same while the $\boldsymbol{P}$ reversal yields the energy differences compatible with that of $E_T - E_A$. When the O atom relaxes above Fe this results in the highly unfavorable configuration F, with the energy of 2.1 eV larger than that of case A. This can be understood by inspecting the relaxed structures of the A and T configurations. These are very similar to that of a O/Fe(001), which were under debate in the literature [25]; the O adatom is relaxed at the hollow site by about 0.3 Å above the Fe ML. The configurations A and T do not differ significantly with respect to each other and with respect to the uncovered 1-ML Fe on ABO_3. In the case of configuration F, the coverage $c = 0.5$ makes the two Fe sites nonequivalent and, as a result, the Fe atom below oxygen moves outward the

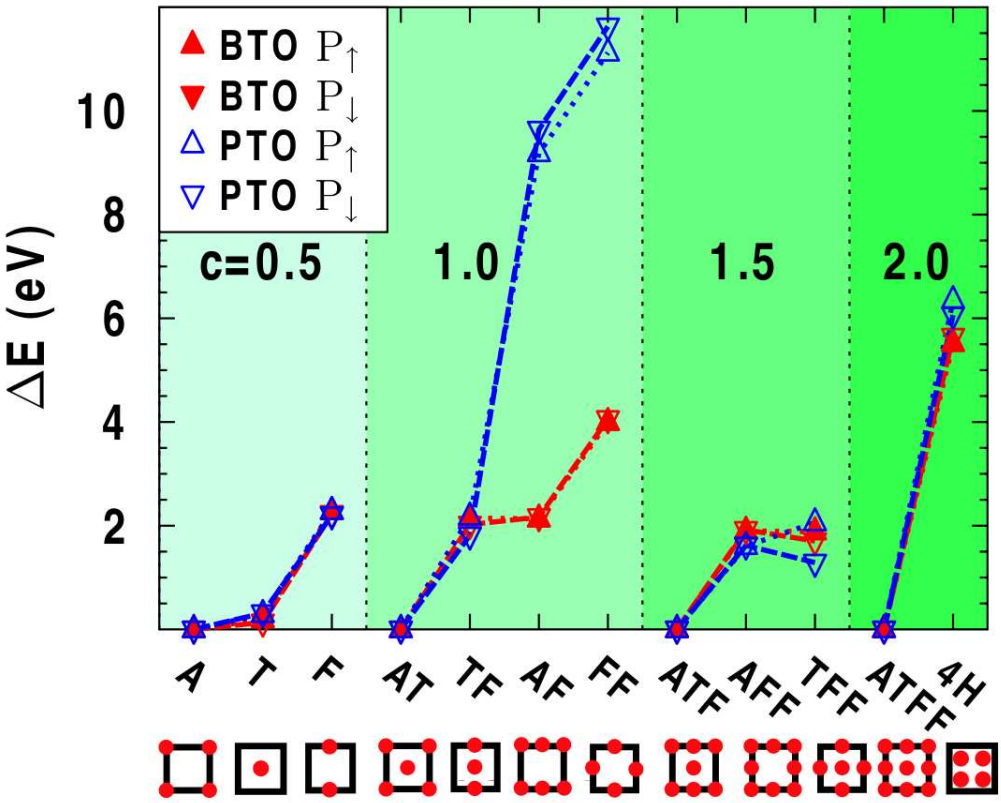

Figure 7: Relaxed total energy of $O_x/Fe_2/ATO(001)$ (A = Ba, Pb and $0 < x < 4$) is plotted for twelve simulated O configurations. The latter are given schematically below the labels. For each coverage c, the configuration with lowest energy pins the energy zero.

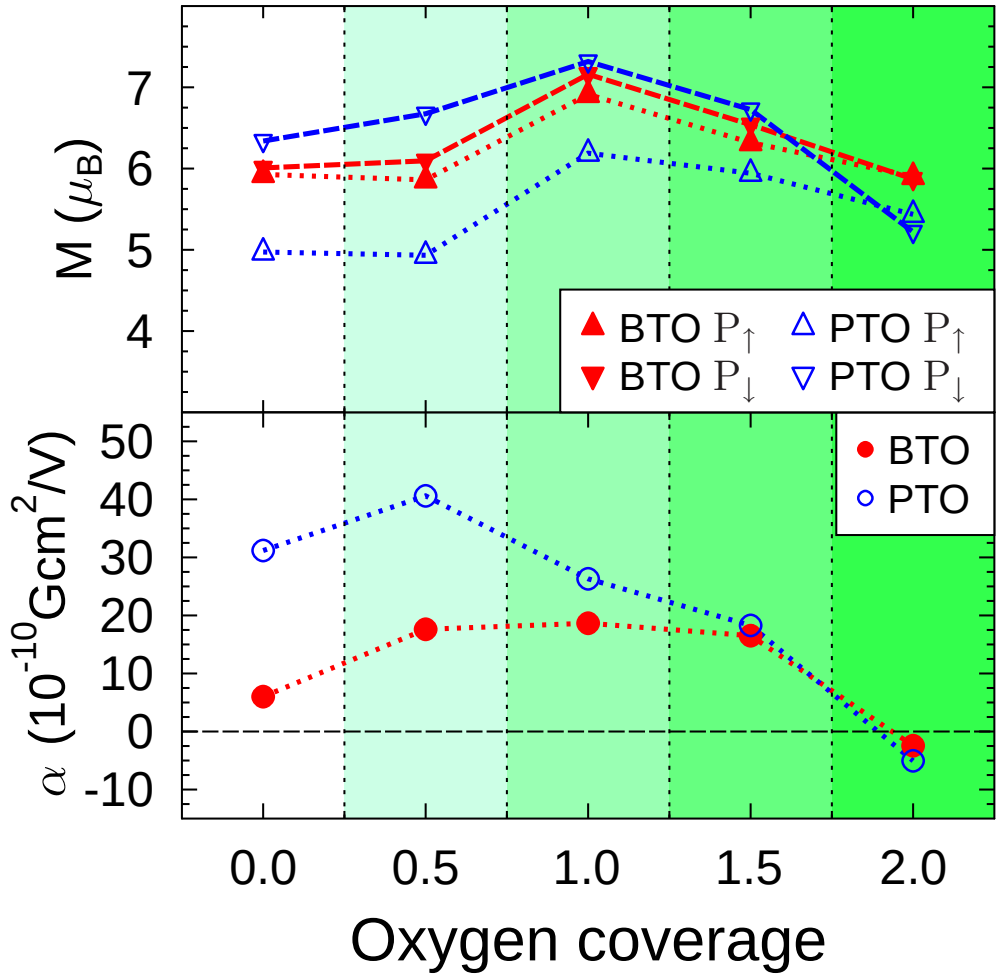

Figure 8: The total magnetization M of $O_x/Fe_2/ATO(001)$ (A = Ba, Pb and $0 < x < 4$) as a function of oxygen coverage is shown in the top panel. For each coverage the energetically favorable configuration was assumed. The magnetoelectric coupling coefficient α is shown in the lower panel.

Fe layer, displacing therefore the O atoms of the interface TiO_2 layer in the same way. The structural distortions make the configuration F energetically unfavorable.

The energetics which is calculated for the coverage $c = 1$ can be explained using our findings for $c = 0.5$. We expect the two O adatoms occupy the positions above A and Ti. Here, $\boldsymbol{P}$ reversal gives a change in energy of about 0.2 eV for both systems. Any of the three other configurations TF, AF or FF always includes at least one energetically unfavorable position atop Fe that drastically increases the associated surface energy. The configuration FF represents the most distorted system whose energy is larger by 12 eV (4 eV) compared to that of the AT configuration of PTO (BTO). For the same reason, the energetically favorable scenario of $c = 1.5$ is the configuration ATF when one site above Fe is empty. Regarding $c = 2$, we have inspected two configurations: ATFF and 4H (shown in Fig. 1). It turns out that the 4H configuration, with all four hollow sites occupied by O, is unfavorable.

In the top panel of Fig. 8 we show the total M, calculated for the lowest energy configuration of $O_x/Fe_2/ATiO_3$ for each O coverage. These are the configurations A, T, AT, ATF and ATFF

obtained for $c = 0.5, 1, 1.5$ and 2, respectively. For $c = 0.5$ we used the average between the A and the T configuration since they can coexist. The magnetization of uncovered Fe/PTO and Fe/BTO is also shown as well. The increase of M seen for $c = 0.5$ and $c = 1$, as compared to that of $c = 0$, is due to a induced magnetic moment at the O adatom which is aligned parallel to the Fe magnetic moment. In the case of low coverage, namely for $c = 0.5$ and $c = 1$, the Fe moment is not affected by the presence of adatoms. Contrarily, when the O adatom relaxes above Fe in the configurations ATF and ATFF, the Fe magnetic moment is decreased by about $1\,\mu_B$. This is mostly due to a relatively small distance between the O adatom and Fe along [001]. As a result, M gradually decreases with increasing $c > 1$.

In summary we demonstrate here that in the case of O/Fe/BTO the magnitude of ΔM remains rather stable for O coverages $c < 1.5$. With further increase of c, $\Delta M \to 0$ at $c = 2$. For the PTO substrate, the trends of ΔM computed for $c > 1.5$ are similar to those of BTO. It should be kept in mind that the dense coverage of $c = 2$ is unrealistic since the highest oxidation state of iron seen in Fe_2O_3 mimics the coverage $c = 1.5$.

The lower panel of Fig. 8 shows the change of the interface ME coupling coefficient, α, which can be evaluated as the ratio of the surface magnetization change $\mu_0 \Delta \boldsymbol{M}/S$ and the coercive field E_c, where S is the interface area. The experimental $E_c = 10\,\mathrm{kV/cm}$ and $E_c = 33\,\mathrm{kV/cm}$ were used for Fe/BTO and Fe/PTO, respectively. In general, the variation of α as a function of c follows the trends of ΔM. However, for $1 < c < 1.5$ we find that the two systems obey almost the same strength of α and, hence, there would be no advantage to use a highly polar PTO substrate for the dense O coverage.

3 Summary

In summary, the magnetism of two-phase multiferroics, realized by ultrathin Fe films on $ATiO_3$ perovskites (A = Ba, Pb, Sr), is found to exhibit a rich and peculiar structure, as is predicted from first-principles computational materials science. A ferromagnetic-to-ferrimagnetic transition which is accompanied by a strong reduction of the Fe magnetic moments could be used in device applications to tailor the properties of the magnetic subsystem. Significant magnetoelectric coupling via the Fe/$ATiO_3$ interface is predicted, a spin-reorientation transition under switching is not found. In view of device applications it appears highly desirable to investigate theoretically and experimentally the thickness-dependent magnetic properties of Fe films sandwiched between ferroelectric perovskites.

Furthermore we discussed the effect of oxidation on the strength of magnetoelectric coupling seen at the biferroic interface in epitaxial ferromagnetic/ferroelectric nanocomposites. The oxygen coverage, ranging between $c = 0.5$ and two adsorbed O per Fe atom were simulated for $O_x/Fe_2/BaTiO_3(001)$ and $O_x/Fe_2/PbTiO_3(001)$ multiferroics. We suggest that oxygen adatoms may find their relaxed positions atop the Ba (Pb) and/or Ti sites. For $c > 1$, the magnetic properties computed for the Fe layer gradually degrade with increasing O coverage. However, when $c < 1.5$ the change in magnetization induced by polarization reversal is robust for all energetically preferable compositions. On the basis of our calculations we, therefore, suggest that intrinsic oxidation of biferroics may not destroy their magnetoelectricity significantly. In the case

of realistic oxygen coverage ($c = 1$), we expect that the strength of magnetoelectric coupling is similar for both biferroic systems under consideration.

References

[1] Hans Schmid. Some symmetry aspects of ferroics and single phase multiferroics. *J Phys-Condens Mat*, 20(43):434201, Jan 2008.

[2] W Eerenstein, M Wiora, J. L Prieto, J. F Scott, and N. D Mathur. Giant sharp and persistent converse magnetoelectric effects in multiferroic epitaxial heterostructures. *Nat Mater*, 6:348–351, Jan 2007.

[3] Sang-Wook Cheong. Transition metal oxides: The exciting world of orbitals. *Nat Mater*, 6:927–928, Jan 2007.

[4] F Zavaliche, T Zhao, H Zheng, F Straub, M. P Cruz, P.-L Yang, D Hao, and R Ramesh. Electrically assisted magnetic recording in multiferroic nanostructures. *Nano Lett*, 7(6):1586–1590, Jan 2007.

[5] G.A. Smolenskii and I.E. Chupis. Ferroelectromagnets. *Sov. Phys. Usp.*, 25:475, 1982.

[6] Daniel Khomskii. Classifying multiferroics: Mechanisms and effects. *Physics*, 2(20):1–8, Mar 2009.

[7] M Fiebig. Revival of the magnetoelectric effect. *J Phys D Appl Phys*, 38(8):R123–R152, Jan 2005.

[8] James M Rondinelli, Massimiliano Stengel, and Nicola A Spaldin. Carrier-mediated magnetoelectricity in complex oxide heterostructures. *Nature Nanotech*, 3:46–50, Jan 2008.

[9] Chun-Gang Duan, Sitaram S Jaswal, and Evgeny Y Tsymbal. Predicted magnetoelectric effect in fe/batio3 multilayers: Ferroelectric control of magnetism. *Phys Rev Lett*, 97:–, Jan 2006.

[10] M Fechner, I. V Maznichenko, S Ostanin, A Ernst, J Henk, P Bruno, and Ingrid Mertig. Magnetic phase transition in two-phase multiferroics predicted from first principles. *Phys Rev B*, 78(21):212406, Jan 2008.

[11] Chengtao Yu, Michael J Pechan, Swedesh Srivastava, Chris J Palmstrom, Michael Biegaslski, Charles Brooks, and Darrell Schlom. Ferromagnetic resonance in ferromagnetic/ferroelectric fe/batio3/srtio3(001). *J Appl Phys*, 103(7):07B108, Jan 2008.

[12] Chun-Gang Duan, Julian P Velev, R. F Sabirianov, W. N Mei, Sitaram S Jaswal, and Evgeny Y Tsymbal. Tailoring magnetic anisotropy at the ferromagnetic/ferroelectric interface. *Appl Phys Lett*, 92(12):122905, Jan 2008.

[13] Manish K Niranjan, Julian P Velev, Chun-Gang Duan, Sitaram S Jaswal, and Evgeny Y Tsymbal. Magnetoelectric effect at the fe_3o_4/$batio_3$ (001) interface: A first-principles study. *Phys Rev B*, 78(10):8, Sep 2008.

[14] C. A. F Vaz, J Hoffman, A.-B Posadas, and C. H Ahn. Magnetic anisotropy modulation of magnetite in fe[sub 3]o[sub 4]/batio[sub 3](100) epitaxial structures. *Appl. Phys. Lett.*, 94(2):022504, Jan 2009.

[15] C Israel, N. D Mathur, and J. F Scott. A one-cent room-temperature magnetoelectric sensor. *Nat Mater*, 7(2):93–94, Jan 2008.

[16] G Kresse and J Furthmüller. Efficient iterative schemes for ab initio total-energy calculations using a plane-wave basis set. *Phys Rev B*, 54:11169–11186, Jan 1996.

[17] M Luders, A Ernst, WM Temmerman, Z Szotek, and PJ Durham. Ab initio angle-resolved photoemission in multiple-scattering formulation. *J Phys-Condens Mat*, 13(38):8587–8606, Jan 2001.

[18] J. Henk, H. Mirhosseini, P. Bose, K. Saha, N. Fomynikh, T. Scheunemann, S. V. Halilov, E. Tamura, and R. Feder. OMNI—Fully relativistic electron spectroscopy calculations, 2008. the computer code is available from the authors.

[19] M Fechner, S Ostanin, and Ingrid Mertig. Effect of the surface polarization in polar perovskites studied from first principles. *Phys Rev B*, 77(9):094112, Jan 2008.

[20] J Henk, AMN Niklasson, and B Johansson. Magnetism and anisotropy of ultrathin ni films on cu(001). *Phys Rev B*, 59(14):9332–9341, Jan 1999.

[21] S Ostanin, SSA Razee, JB Staunton, B Ginatempo, and E Bruno. Magnetocrystalline anisotropy and compositional order in fe0.5pt0.5: Calculations from an ab initio electronic model. *J Appl Phys*, 93(1):453–457, Jan 2003.

[22] JB Staunton, S Ostanin, SSA Razee, BL Gyorffy, L Szunyogh, B Ginatempo, and E Bruno. Temperature dependent magnetic anisotropy in metallic magnets from an ab initio electronic structure theory: L1(0)-ordered fept. *Phys Rev Lett*, 93(25):257204, Jan 2004.

[23] TC Leung, CT Chan, and BN Harmon. Ground-state properties of fe, co, ni, and their monoxides - results of the generalized gradient approximation. *Phys Rev B*, 44(7):2923–2927, Jan 1991.

[24] HJ Monkhorst and JD Pack. Special points for brillouin-zone integrations. *Phys Rev B*, 13:5188–5192, Jan 1976.

[25] RQ Wu and AJ Freeman. Magnetism of fe on w(oo1) and the effects of oxygen-adsorption. *J Magn Magn Mater*, 127(3):327–345, Jan 1993.